Nanoscale

Sub-diffractional waveguiding by mid-infrared plasmonic resonators in semiconductor nanowires

Journal:	*Nanoscale*
Manuscript ID	NR-ART-01-2018-000701.R1
Article Type:	Paper
Date Submitted by the Author:	06-Mar-2018
Complete List of Authors:	Tervo, Eric; Georgia Institute of Technology, George W. Woodruff School of Mechanical Engineering Boyuk, Dmitriy; Georgia Institute of Technology, School of Chemical and Biomolecular Engineering Cola, Baratunde; Georgia Institute of Technology, George W. Woodruff School of Mechanical Engineering; Georgia Institute of Technology, School of Materials Science and Engineering Zhang, Zhuomin; Georgia Institute of Technology, Mechanical Engineering Filler, Michael; Georgia Institute of Technology, School of Chemical and Biomolecular Engineering

Nanoscale

PAPER

Sub-diffractional waveguiding by mid-infrared plasmonic resonators in semiconductor nanowires†

Received 00th January 20xx,
Accepted 00th January 20xx

DOI: 10.1039/x0xx00000x

www.rsc.org/

Eric J. Tervo,[a] Dmitriy S. Boyuk,[b] Baratunde A. Cola,[a,c] Zhuomin M. Zhang,*[a] and Michael A. Filler *[b]

Chains of nanoscale plasmonic resonators are capable of sub-diffractional waveguiding and have applications in nanophotonics and thermal radiation transport. Practical uses have largely been limited, however, due to high optical losses or low group velocities. Here, we predict the waveguide performance of a material structure capable of overcoming these limitations: plasmonic resonators embedded in high-dielectric nanowires. Due to the enhanced near-field coupling between resonators, we find that the group velocities and propagation lengths for doped Si plasmonic resonators in intrinsic Si nanowires can be increased by up to an order of magnitude compared to the case of isotropic vacuum surroundings. We investigate the impact of resonator aspect ratio, doping, and spacing on waveguide performance, and we find that propagation lengths are maximized for large aspect ratios and high dopant concentrations at small spacings. To study these complex anisotropic systems, we develop a new analytical "absorption spectra" method to extract waveguide information from simple far-field absorption experiments (or simulations) of only two coupled resonators.

Introduction

Collective, resonant charge oscillations in nanoparticles, known as localized surface plasmon polaritons (SPPs) in metals and localized surface phonon polaritons (SPhPs) in polar dielectrics, can confine light to volumes far below the diffraction limit. In addition to applications in chemical sensing,[1] energy conversion,[2] and photocatalysis,[3] among others,[4] nanoscale polaritonic particles may serve as sub-diffractional waveguides for nanophotonic devices when organized into extended one-dimensional arrays.[5-10] These types of particle chains also have the potential for enhanced, guided near-field thermal radiation if designed for the mid- or far-infrared.[11-15] The ability to confine and transmit light at such small dimensions has important implications for photonic circuits,[16] plasmonic sensing,[17] and other optical applications. However, the performance of nanoparticle chain waveguides has been limited when compared to plasmonic nanowires[18] or hybrid plasmonic-photonic waveguides[19] due to inherent losses in metal-based SPPs[20] and strong dispersions (corresponding to low group velocities) for SPhPs in polar dielectrics.[21]

One way to mitigate these waveguide limitations may be to utilize anisotropy and polarizable materials along the nanoparticle chain. For doped Si plasmonic resonators embedded in an intrinsic Si nanowire, the near-field coupling strength between two resonators is enhanced by four to five times compared to the same resonators in isotropic vacuum or in isotropic intrinsic Si.[22] This behaviour is caused by the combination of the anisotropic structure of the nanowire and intrinsic Si's large infrared permittivity, which focuses the electric field along the nanowire and suppresses transverse modes. If the resonators are repeated along the wire to create a sub-diffractional waveguide, they could exhibit good waveguide performance due to the improved coupling strength. A conceptual schematic of this type of waveguide is shown in Fig. 1, where the coloured shading represents the local electric field intensity and the sine wave represents one frequency's contribution to the propagating SPP or SPhP wave at a certain point in time. Additional benefits of these types of waveguides are their ability to be fabricated through bottom-up synthesis methods,[22-25] which lend themselves to high throughput production, and the ability to tune waveguide properties through chemical doping, electrostatic gating, and/or optical excitation of carriers.

[a] George W. Woodruff School of Mechanical Engineering, Georgia Institute of Technology, Atlanta, Georgia 30332, United States. E-mail: zhuomin.zhang@me.gatech.edu
[b] School of Chemical and Biomolecular Engineering, Georgia Institute of Technology, Atlanta, Georgia 30332, United States. E-mail: mfiller@gatech.edu
[c] School of Materials Science and Engineering, Georgia Institute of Technology, Atlanta, Georgia 30332, United States.
†Electronic Supplementary Information (ESI) available. See DOI: 10.1039/x0xx00000x

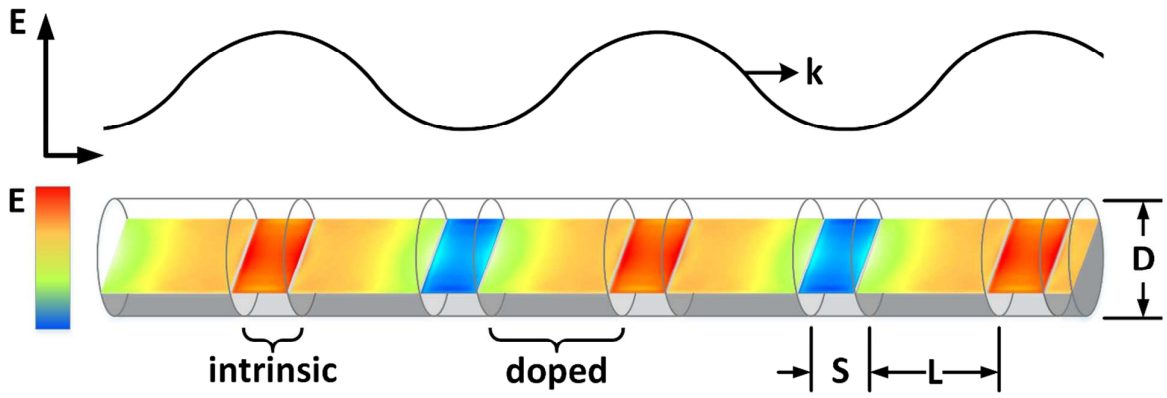

Fig. 1 Schematic of a sub-diffractional waveguide consisting of repeated plasmonic doped semiconductor resonators (dark grey) embedded in an intrinsic semiconductor nanowire (light grey). The resonators have length L, diameter D, aspect ratio $AR = L/D$, separation distance S, and center-to-center spacing $d = L + S$. External excitations cause surface modes to couple across multiple resonators, resulting in alternating regions of high (red) and low (blue) electric field intensity E. The waveguide modes move along the chain as propagating waves with a wavevector k, represented by the sine wave above the nanowire.

Understanding and analysing the behaviour of nanowire waveguides is made challenging by the nonhomogeneous environment around the resonators. Since the prediction of sub-diffractional waveguiding along nanoparticle chains by Quinten *et al.* in 1998,[5] the concept has been theoretically investigated by applying Maxwell's equations through the use of Mie theory,[5] equations of motion for coupled dipole oscillation,[6] and wave solutions to coupled electric field interactions,[8] to name a few methods. Good reviews on the topic are available by Gramotnev and Bozhevolnyi[9] and by Halas *et al.*[10] The approach of finding wave solutions to the coupled electric field interactions is also used to predict near-field radiation heat transfer along nanoparticle chains.[11-13] In general, these methods calculate the dispersion relation for the propagating SPhP or SPP modes and then use the dispersion to predict mode propagation lengths, group velocities, and thermal transport. For example, Brongersma *et al.* showed that the dispersion relation depends on a parameter called the "coupling strength" between any two resonators,[6] which can be directly calculated from electromagnetic source-field relations. Most analytical approaches rely on such equations, but these are not generally known for particles in anisotropic environments and must instead be obtained through numerical methods. An alternative approach is therefore needed that does not rely on source-field relations.

In this paper, we develop a new method to calculate the dispersion relation for SPPs or SPhPs propagating along a chain of resonators from common far-field spectral response measurements or numerical simulations of two coupled resonators. The shift in absorption peak position as two resonators are brought closer together is used to find the coupling strength between resonators in the waveguide chain. The coupling strength is used in an equation of motion approach to calculate the dispersion relation, which provides mode group velocities and propagation lengths. We term this approach the "absorption spectra method" and use it to predict the waveguide performance of doped Si plasmonic resonators embedded in intrinsic Si nanowires. Dispersion characteristics are compared to the case of the same resonators embedded in an isotropic vacuum environment to quantify the improvements associated with the nanowire geometry. Finally, we investigate the impacts of resonator aspect ratio, spacing, and doping to guide the design of future waveguides.

Theory

Dispersion Relation

Consider a chain of identical plasmonic resonators modelled as dipoles with center-to-center spacing d. If the resonators are SPP- or SPhP-supporting spherical nanoparticles, then the dipolar assumption is valid when d is approximately greater than or equal to three times the particle radius.[26, 27] For doped Si plasmonic resonators embedded in semiconductor nanowires, the transverse modes are strongly suppressed and longitudinal oscillatory behaviour remains dipolar even at very close resonator spacings.[22, 25, 28] Following the example of Brongersma *et al.*,[6] we model the dipolar resonators as harmonic oscillators[29] with displacement $\mathbf{x}$, restoring force spring constant K, effective mass m, and damping coefficient Γ. A polarized dipole in the chain will create an electric field at the neighboring dipoles that exerts a force proportional to the dipole displacement $F = Bx$, where we drop the vector notation for $\mathbf{x}$ because only 1D longitudinal polarization is considered. This leads to an equation of motion for the nth resonator in the chain:

$$\sum_{l=1}^{N} \omega_{c,l}^2 (p_{n-l} + p_{n+l}) = \frac{d^2 p_n}{dt^2} + \xi \frac{dp_n}{dt} + \omega_0^2 p_n \qquad (1)$$

where N is the number of neighboring resonators considered and t is time. We have also introduced the coupling strength of the lth neighbors with the nth resonator $\omega_{c,l} = \sqrt{B_l/m}$, the

dipole moment $p = qx$ where q is the charge, the damping ratio $\xi = \Gamma/m$, and the natural frequency $\omega_0 = \sqrt{K/m}$. The left side of eqn (1) represents the force on the nth resonator due to the polarization of all other resonators, and the right side encompasses the motion and forces associated with the oscillation of the nth resonator. We assume the form of a complex frequency $\tilde{\omega} = \omega + i\zeta$ such that ω is the angular frequency and ζ is the damping rate,[8] and we look for propagating wave solutions to eqn (1) of the form $p_{n\pm l} = Pe^{-\zeta t - i[k(n\pm l)d - \omega t]}$ where P is the amplitude and k is the wavevector. After inserting this into eqn (1), simplifying, and separating the real and imaginary parts, we obtain the dispersion relation

$$0 = \omega^2 - \zeta(\zeta - \xi) - \omega_0^2 + 2\sum_{l=1}^{N} \omega_{c,l}^2 \cos(kld) \quad \text{(Real)} \tag{2a}$$

$$0 = 2\zeta - \xi \quad \text{(Imaginary)} \tag{2b}$$

A more detailed derivation of the dispersion relation is provided in Section S1 of the ESI†. Equation (2) provides a relation between k, ω, and ζ that depends only on the spacing d, the coupling strength $\omega_{c,l}$ for each term in the summation, the natural frequency ω_0, and the damping ratio ξ. The imaginary part of the solution verifies the typical relationship between the damping rate and the damping ratio, $\zeta = \xi/2$.

The dispersion relation is the key to defining waveguide performance with the following steps. The parameters in eqn (2) are first determined, as described in the following section, through spectral response measurements or numerical simulations. Once the inputs have been specified, k is varied from zero to the first Brillouin zone π/d to find the corresponding values of ω. With the dispersion then determined, the group velocity $v_g = \frac{d\omega}{dk}$ and the amplitude propagation length (1/e length) $\Lambda = v_g/\zeta$ are calculated to evaluate spectral waveguide performance.[8]

Damping Ratio, Natural Frequency, and Coupling Strength

The first two inputs, ξ and ω_0, are associated with the oscillation of single resonator. These inputs are therefore determined from the absorption spectrum of an isolated particle in the background material being considered for the waveguide (e.g., a nanowire). Because a localized SPP or SPhP can be modelled as a damped harmonic oscillator driven by the incident light, ξ is simply the full-width at half maximum[30] and ω_0 is the absorption peak frequency for the isolated resonator.[29] To determine the coupling strength between two resonators, ω_c, we consider the coupled equation of motion for two particles, designated a and b, driven longitudinally by the incident light:

$$\frac{2F_0}{m}e^{i\omega t} + \omega_c^2 z = \frac{d^2z}{dt^2} + \xi\frac{dz}{dt} + \omega_0^2 z \tag{3}$$

Here $z = x_a + x_b$ is the sum of the displacement of the oscillators, the sinusoidal driving force $F(t)$ is represented by $F_0e^{i\omega t}$, and the real part of the solution $z(t) = Ce^{i\omega t}$ represents the physical motion. The absorption peak frequency for the two-resonator system, ω_2, which can be experimentally measured or simulated, corresponds to the frequency at which the average power is delivered to the resonators is maximized. After solving for C in the solution $z(t)$, this average power is given by

$$\langle \dot{W}(t) \rangle = \langle F(t)\frac{dz}{dt} \rangle = \frac{F_0^2}{\xi m} \cdot \frac{\xi^2\omega^2}{\xi^2\omega^2 + (\omega_0^2 - \omega_c^2 - \omega^2)^2} \tag{4}$$

The absorption peak frequency is found by setting the derivative of eqn (4) with respect to ω equal to zero and solving for ω. This leads to the relation

$$\omega_2 = \sqrt{\omega_0^2 - \omega_c^2} \tag{5}$$

The coupling strength between two resonators may, therefore, be determined knowing only the natural frequency (which is the same as the absorption peak frequency for an isolated resonator) and the absorption peak frequency of the two resonators in proximity to each other. A more detailed derivation of this relation is provided in Section S2 of the ESI†.

Instead of performing measurements or simulations to obtain the absorption peak shift for all N resonator spacings in eqn (2), it is more efficient to only do so for a few spacings and then interpolate the others. The shift in absorption peak position with spacing for two plasmonic resonators is correlated by the empirical plasmon ruler equation,[31] which is known to be valid for coupled resonators in both isotropic[32-36] and anisotropic[22, 31, 37-39] environments:

$$\frac{\omega_2 - \omega_0}{\omega_0} = A_0 \exp\left(-\frac{S/L}{\tau}\right) \tag{6}$$

where A_0 is a dimensionless constant, S is the separation distance between the resonators, L is the length of the resonators, and τ is the decay length scaling factor. τ indicates the rate at which the electric field decays away from the resonator, so larger values of τ are linked to stronger near-field coupling. Once absorption peak locations have been obtained for several different resonator spacings, the data may be fit to eqn (6) to obtain values for A_0 and τ. Despite its empirical nature, the exponential behavior of the shift in absorption peak may also be explained by a dipolar coupling model: as the resonators move closer or exert stronger fields on each other due to changes in geometry or material properties, the coupling strength between them also increases.[31]

Summary of Method

For clarity, we summarize here the steps in the absorption spectra method to calculate the dispersion relation. First, measurements or simulations of the far-field absorption peak position and width of an isolated resonator in the background

medium of interest provide ω_0 and ξ. Additional far-field measurements or simulations for two coupled resonators at several different spacings then provide several values for ω_2. These data are fit to eqn (6) to obtain A_0 and τ, which allows the calculation of ω_2 for any resonator spacing. Second, eqn (6) and eqn (5) are used repeatedly to calculate N values of ω_c for N neighboring resonators. The coupling strength decays rapidly with increased spacing, so typically $N < 10$ is sufficient. The requirement for N will vary with material, geometry, and environment, so this should be checked for any specific application. Finally, k is varied from 0 to π/d and eqn (2) is solved for each value of k, which provides the dispersion relation. With the dispersion, the mode v_g and Λ may be calculated to evaluate waveguide performance.

Validation

To verify that our method provides a good prediction of waveguide properties, we compare its results for spherical nanoparticle chains in homogeneous dielectric environments to analytical solutions for the same materials and geometries. Absorption spectra for 12 nm diameter nanoparticles were calculated using the discrete dipole approximation (DDA) with the well-established DDSCAT code.[40] The spectra for SiC particles and SiO_2 particles in background permittivities of ε_m = 1 and ε_m = 4, respectively, are shown in Fig. S1 of the ESI†. For both materials, a Lorentz oscillator model for relative permittivity was fit to the optical constants[41] in the SPhP resonance spectral region, and this model was used to describe the particle permittivity for all scattering and dispersion calculations. The absorption spectra for a single nanoparticle provided the full-width at half maximum or damping ratio (ξ = 1.06×10^{12} rad/s for SiC; ξ = 1.62×10^{12} rad/s for SiO_2) as well as the absorption peak frequency or natural frequency (ω_0 = 1.75×10^{14} rad/s for SiC, ω_0 = 2.09×10^{14} rad/s for SiO_2). The DDA results for a single nanoparticle were also shown to be consistent with Mie theory (Supplementary Information Fig. S1 and S2).[26, 42] The absorption peak frequencies for two particles separated by distances of 4, 6, 8, and 10 nm were then used to fit the values of τ and A_0 in the plasmon ruler eqn (6) (τ = 0.422, A_0 = 0.0143, R^2 = 99.2% for SiC; τ = 0.471, A_0 = 0.00881, R^2 = 99.5% for SiO_2). With the plasmon ruler equation we can specify the peak absorption frequency for two resonators at an arbitrary separation distance, which allowed us to calculate the coupling strength for N neighboring resonators with the repeated use of eqn (6) and eqn (5). Once all inputs were determined, eqn (2) was solved using a custom MATLAB code using d = 18 nm and N = 15 to find the dispersion relations and propagation lengths for SiC and SiO_2 nanoparticle chains, shown by the solid lines in Fig. 2a and Fig. 2b. The corresponding analytical solutions were obtained from the longitudinal dispersion relation for an infinite chain of point dipoles:[8]

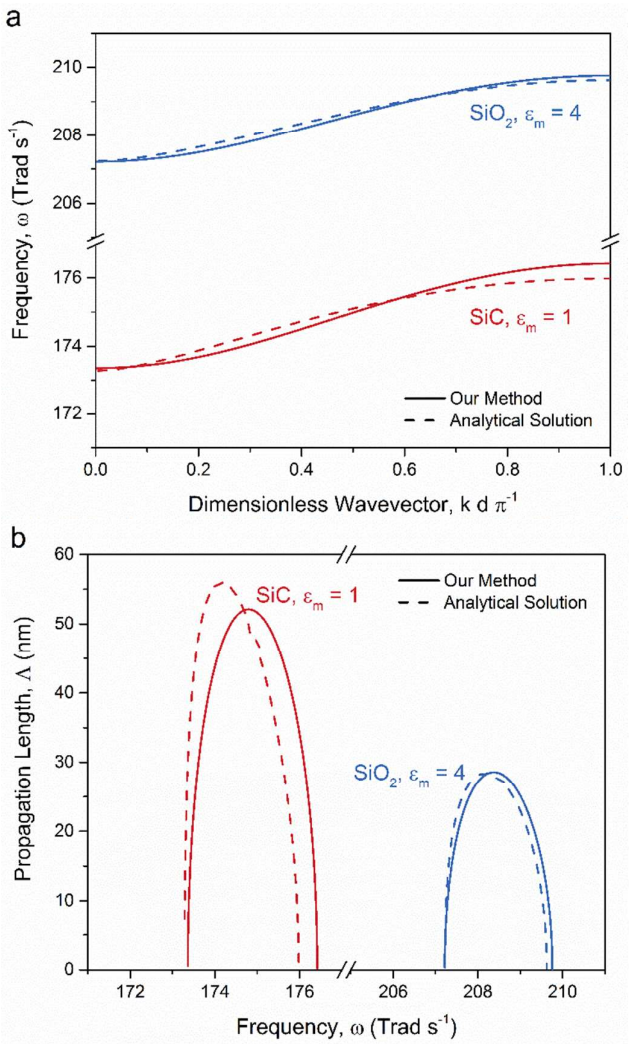

Fig. 2 (a) Dispersion relations and (b) propagation lengths for chains of 12 nm diameter particles with separation distances of 6 nm for SiC in background ε_m = 1 (red lines) and SiO_2 in background ε_m = 4 (blue lines). Our method described in the present work (solid lines) has good agreement with the analytical solution (dashed lines), indicating that the new method can predict the waveguide properties of repeated plasmonic resonators for different materials and environments.

$$0 = 1 - \frac{\alpha}{2\pi\varepsilon_m d^3}\left\{\left[\mathrm{Li}_3\left(e^{i(\tilde{\omega}/v+k)d}\right) + \mathrm{Li}_3\left(e^{i(\tilde{\omega}/v-k)d}\right)\right] - \frac{i\omega d}{v}\left[\mathrm{Li}_2\left(e^{i(\tilde{\omega}/v+k)d}\right) + \mathrm{Li}_2\left(e^{i(\tilde{\omega}/v-k)d}\right)\right]\right\} \quad (7)$$

where α is the nanoparticle polarizability corrected for radiation damping,[26] $\mathrm{Li}_m(\cdots)$ is the polylogarithm function of order m, and $v = c/\sqrt{\varepsilon_m}$ where c is the speed of light in vacuum. Equation (7) was solved numerically in MATLAB and the results are shown by the dashed lines in Fig. 2a and Fig. 2b. The dispersion relations provide the relationship between the wavevector and frequency for the allowed propagating modes. The propagation lengths reach a maximum where the group velocity (slope of the dispersion) is largest.

Both the dispersion relations and the propagation lengths calculated with the absorption spectra method agree well with the analytical solutions. The dispersion relations differ from the analytical solutions within 0.23%, and the maximum propagation lengths differ from the analytical solutions by 6.8% for SiC and 0.8% for SiO_2. The consistent shapes of the dispersions and close accuracy to the analytical solutions regardless of material or background permittivity show that our method can account for these variations.

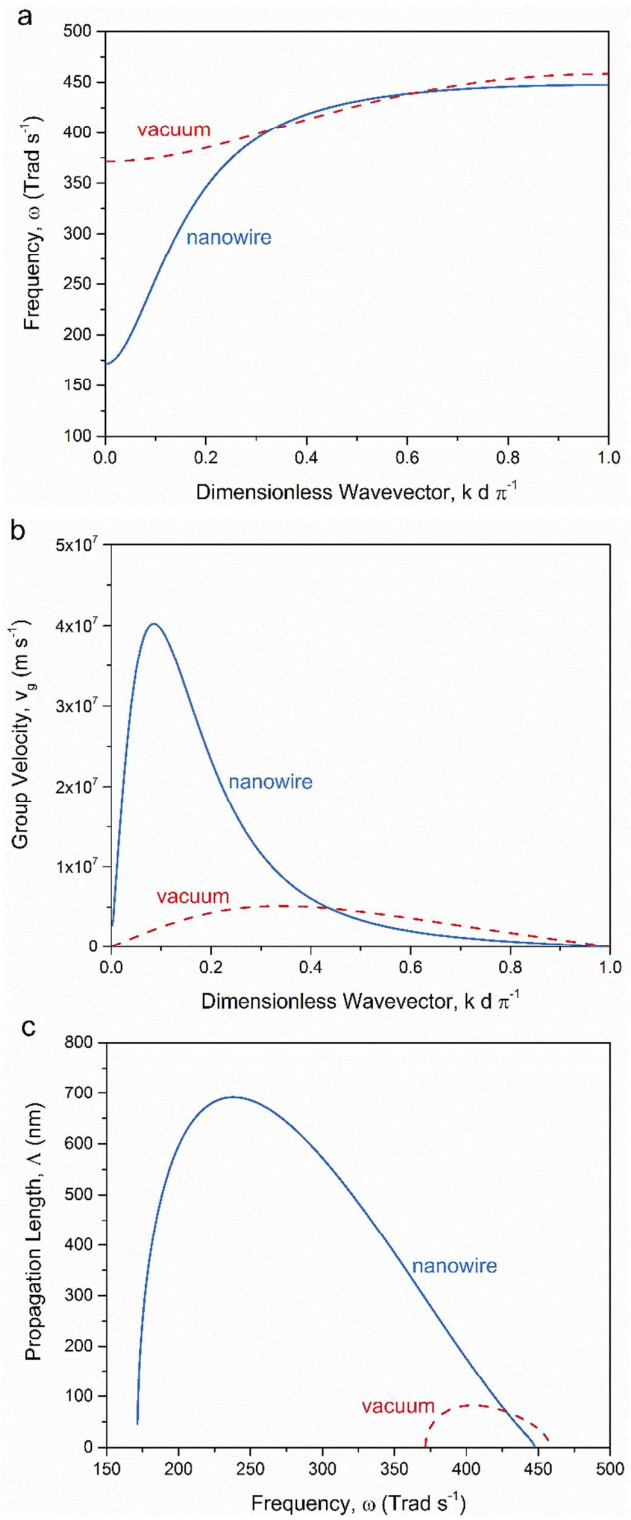

Fig. 3 (a) Dispersion relations, (b) group velocities, and (c) propagation lengths for doped Si plasmonic resonators in isotropic vacuum (red dashed lines) and embedded in an intrinsic Si nanowire (solid blue lines). Stronger coupling between the resonators embedded in the nanowire leads to higher group velocities and propagation lengths, therefore the nanowire environment exhibits superior waveguide properties.

Results and Discussion

The proposed absorption spectra method was used to predict the waveguide performance of chains of doped Si plasmonic resonators embedded in intrinsic Si nanowires. First, DDA simulations from our previous work[22] were used as inputs to evaluate how the nanowire medium affects the group velocities and propagation lengths when compared to a homogeneous vacuum environment. Waveguide performance modelled from experimental spectral response measurements were compared to performance modelled from the DDA simulations to determine how a real system differs from idealized simulations. Finally, new DDA simulation results were used to investigate the impact of resonator size, spacing, and dopant concentration.

Impact of the Nanowire Environment

DDA simulations for doped Si plasmonic resonators with a doping concentration N_e of 2.7×10^{20} cm^{-3},[43] diameter of 130 nm, and aspect ratio of 0.77 provided values for ω_0, ξ, and ω_2 for both isotropic vacuum and intrinsic Si nanowire environments.[22] The resulting dispersion relations, group velocities, and propagation lengths for this nanowire structure are shown in Fig. 3a, 3b, and 3c, respectively, for N = 15 nearest neighbours and a separation distance of 10 nm between adjacent resonators.

The anisotropic nanowire environment, as expected,[22] alters the coupling between resonators and the waveguide characteristics significantly compared to the isotropic vacuum environment. Fig. 3a shows that the nanowire dispersion exhibits steeper slopes and covers a broader frequency range, which translates to much higher group velocities in Fig. 3b. Because the damping does not change significantly between the two environments (ξ = 1.16×10^{14} rad/s for the nanowire case and ξ = 1.24×10^{14} rad/s for the vacuum case), higher group velocities directly lead to greater propagation lengths as shown in Fig. 3d. The maximum propagation length for the nanowire geometry is about eight times higher than that for the vacuum environment, but different resonator geometries or dopant concentrations can exhibit even larger waveguide performance enhancements. For example, based on additional DDA calculations, we found a maximum propagation length of 1.01 μm for resonators with N_e = 1×10^{21} cm^{-3}, diameter of 150 nm, aspect ratio of 0.8, and separation distance of 10 nm. This represents an order of magnitude increase over the case of the same resonators in a vacuum environment.

Inputs from Measurement vs. Simulation

A significant advantage of the absorption spectra method of calculating dispersion relations is that it can use experimental measurements to predict dispersion relations. Such spectral response measurements capture the effects of nonidealities such as defects and dopant concentration gradients, and they give a better indication of real-world coupling strength than

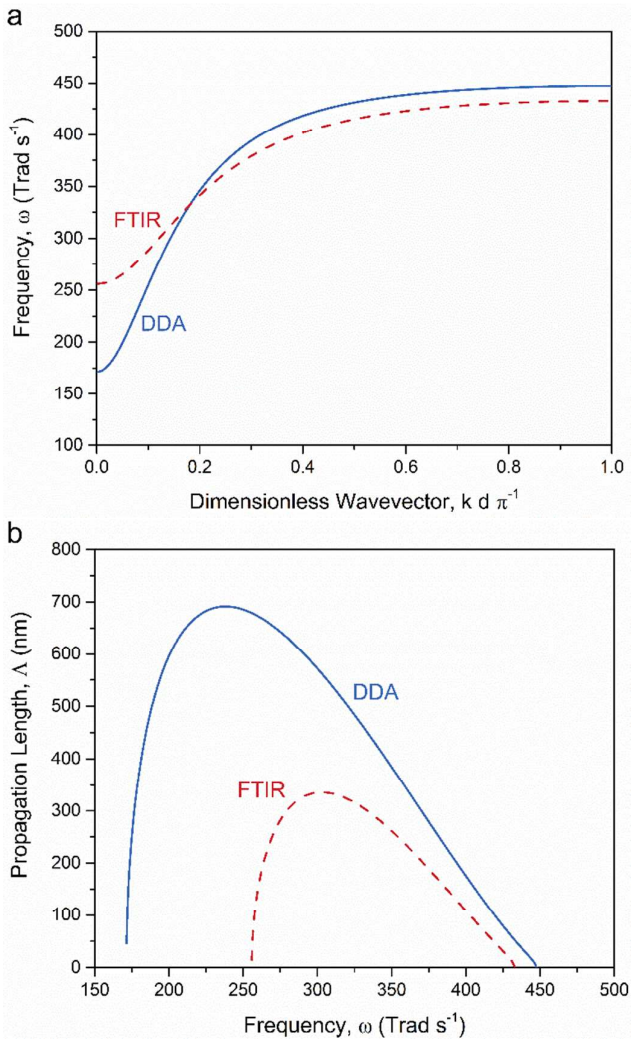

Fig. 4 (a) Dispersion relations and (b) propagation lengths modelled using inputs from FTIR spectroscopy measurements (red dashed lines) and from DDA simulations (blue solid lines). Although the same dopant concentrations and geometries are used in both cases, nonidealities of the physical resonators cause them to exhibit different dispersive behaviour and shorter propagation lengths than the simulated resonators.

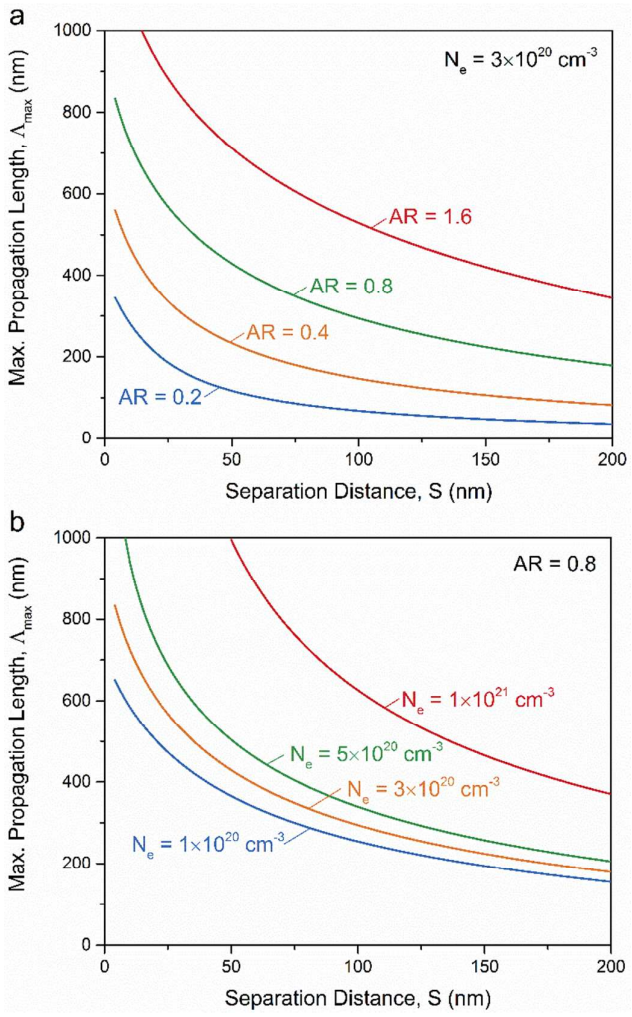

Fig. 5 Impact of resonator separation distance on propagation length for different (a) aspect ratios and (b) dopant concentrations. The largest maximum propagation lengths are obtained for large aspect ratios and high dopant concentrations at small resonator spacings.

numerical simulations may provide. To illustrate how measurements may lead to different results than DDA simulations, we compared waveguide predictions using experimental Fourier-transform infrared (FTIR) spectroscopy measurements to predictions using DDA simulations for the same resonator properties and geometries as discussed in the previous section.[22] The resulting dispersion relations and propagation lengths are shown in Fig. 4a and 4b, respectively.

Although measurements and simulations yielded similar inputs for the dispersion model (τ = 1.34, A_0 = 0.0886, ω_0 = 3.93×10^{14} rad/s, ξ = 1.16×10^{14} rad/s from FTIR measurements and τ = 1.70, A_0 = 0.106, ω_0 = 4.01×10^{14} rad/s, ξ = 1.16×10^{14} rad/s from DDA simulations), we see from Fig. 4 that the differences are enough to cause substantial variation in waveguide properties. Stronger coupling in the DDA case causes a steeper dispersion and a maximum propagation length about double that predicted from the FTIR case. Because the input parameters for the DDA calculations were selected to match the experiments, the differences in Fig. 4 suggest that nonidealities in the growth or measurement processes (e.g., inhomogeneous broadening due to a distribution of nanowire diameters and thus resonator aspect ratios) are responsible for about a 50% reduction in peak propagation length. These differences highlight the importance and usefulness of utilizing experimental spectral response measurements, when possible, to predict the waveguide properties.

Dependence on Resonator Properties and Spacing

DDA simulations are useful to quickly evaluate different materials, geometries, and properties of resonator waveguides, even though they may not capture the nonidealities that exist in real devices. We performed DDA simulations on resonators with different dopant concentrations, aspect ratios, and spacings to elucidate the impacts of these parameters on waveguide performance.

Starting with the baseline properties of N_e = 3×10^{20} cm^{-3}, AR = 0.8, and a diameter of 150 nm, we varied the spacing for different values of N_e and AR while holding other properties constant. The resulting maximum propagation lengths are shown in Fig. 5a for different aspect ratios and Fig. 5b for different dopant concentrations.

Several interesting trends can be seen by examining Fig. 5. First, we observe the known effect that a larger spacing between resonators results in lower propagation lengths regardless of the other resonator properties. This is because the benefits of lower loss with larger spacing are always outweighed by a the exponentially decreasing coupling strength with larger spacing.[31] However, the anisotropic nanowire environment shifts all curves to longer propagation lengths than would be obtained in an isotropic environment. Second, we see in Fig. 5a that higher aspect ratios lead to longer propagation lengths for the same resonator spacing. This is somewhat surprising, considering low aspect ratios result in high decay length scaling factors, which is typically associated with high coupling strength.[22] Larger aspect ratios are also associated with a substantial increase in A_0 and a decrease in S/L in the plasmon ruler equation, which together drive a large absorption peak shift corresponding to a high coupling strength. Third, Fig. 5b shows that a higher dopant concentration causes larger propagation lengths for the same resonator spacing. In this case, the higher charge density results in stronger electric fields associated with the plasmon oscillation. This increases both τ and A_0 in the plasmon ruler equation, and the enhanced coupling strength is enough to outweigh the negative effects of stronger damping with increased dopant concentration. A final important feature of Fig. 5b to note is that the curve for the highest dopant concentration, N_e = 1×10^{21} cm^{-3}, has a lower limit for spacing of about 50 nm, while the other cases all contain data down to about 10 nm spacing. This is because, for this dopant concentration, below 50 nm the dispersion curve becomes so steep that group velocities exceed the speed of light in intrinsic Si, as shown in Fig. S3 of the ESI†. These steep portions of the dispersion were removed from the data to avoid inflated propagation lengths, but they should be examined carefully in future work to determine their origin and significance.

Outlook and Future Work

The proposed absorption spectra method to predict dispersion characteristics offers two opportunities to advance sub-diffractional waveguide performance. First, the ability to quickly simulate absorption and scattering spectra with readily available code such as DDSCAT, in conjunction with our model, means that different resonators and environments may be efficiently tested and optimized for desired waveguide properties. This process may be performed for arbitrarily complex resonator geometries and environments, with the only limitation being computation of the absorption and scattering from pairs of resonators. Second, the ability to use experimental spectral response data for two coupled resonators to calculate the dispersion allows any nonidealities or other physical system effects to be captured in the model. Using both experimental and simulation data may allow researchers to quantify the impact of experimental defects or other features not included in simulations.

A future area of improvement for the model is to develop a better understanding of dispersion behaviour for resonators with very strong coupling. As discussed in the previous section, this results in excessively steep dispersion relations at small frequencies and wavevectors. It is difficult to analyse our model in these regions because analytical comparisons are not available. The system we used for validation of our model, nanoparticle chains in the dipolar limit, does not have strong enough coupling to create these very steep dispersions. More complex electromagnetic numerical simulations may be able to address this open question.

The resonators investigated in this work, plasmonic doped semiconductors, may present interesting opportunities to tune and control waveguide behaviour due to their many adjustable characteristics. In addition to the role of aspect ratio and spacing examined here, more complex geometrical features can be investigated.[22, 44] In the case of semiconductors, it is also possible to actively tune plasmon resonances via electric field[45, 46] or light illumination,[47] which could allow active modulation of waveguide performance. While doped Si was examined here, resonators made from other III-V semiconductors with lower damping rates[48] could significantly increase waveguide propagation lengths,[49] and polar III-V semiconductors could offer waveguiding by SPhPs instead of SPPs.[21] Additionally, the potential for high fabrication throughput via bottom-up synthesis holds promise for much simpler and lower-cost waveguides than top-down synthesized waveguides may allow. Bottom-up synthesis also provides access to structures that may not be fabricated through top-down methods, such as hybrid III-V/IV nanowires.[50]

Although we have focused on the waveguide characteristics of group velocity and propagation length in this work, future investigations will examine thermal energy transport in analogous waveguides. Low-energy resonances and low damping rates could enable thermal excitation of propagating polariton modes, allowing arrays of nanowire waveguides to serve as high thermal conductivity thermal interface materials or guides for near-field thermal radiation. These applications would also benefit from the scalability available with bottom-up synthesis, as large-area devices are required for most thermal applications.

Conclusions

We develop a methodology to predict the sub-diffractional waveguide performance for chains of SPP- or SPhP-supporting nanoscale resonators in arbitrary nonhomogeneous environments using experimental or simulated spectral response data. Our method presents opportunities to analytically examine the dispersion relations, group velocities, and propagation lengths for waveguides that were not accessible through previous methods. Application of our

method to doped Si plasmonic resonators embedded in intrinsic Si nanowires shows that propagation lengths can be increased by up to an order of magnitude compared to the same resonators in an isotropic vacuum. We also show that results differ when using simulated and experimental spectra, which allows the effect of non-idealities present in physical systems to be quantified. The highest propagation lengths are found for large aspect ratios and high dopant concentrations at small resonator spacings. Future work should examine other materials, geometries, and methods to actively tune waveguide performance as well as evaluate the ability to transport thermal energy.

Conflicts of interest

The authors declare no competing financial interest.

Acknowledgements

E.J.T. acknowledges support by the National Science Foundation Graduate Research Fellowship Program under Grant No. DGE-1650044. Any opinions, findings, and conclusions or recommendations expressed in this material are those of the authors and do not necessarily reflect the views of the National Science Foundation. D.S.B. and M.A.F. acknowledge support from the National Science Foundation (no. 1510934) and the GT-FIRE program at Georgia Tech. Z.M.Z. acknowledges support from the U.S. Department of Energy, Office of Science, Basic Energy Sciences (DE-SC0018369).

References

1. K. M. Mayer and J. H. Hafner, *Chemical Reviews*, 2011, **111**, 3828-3857.
2. S. V. Boriskina, H. Ghasemi and G. Chen, *Materials Today*, 2013, **16**, 375-386.
3. S. Linic, U. Aslam, C. Boerigter and M. Morabito, *Nature Materials*, 2015, **14**, 567-576.
4. J. A. Schuller, E. S. Barnard, W. Cai, Y. C. Jun, J. S. White and M. L. Brongersma, *Nature Materials*, 2010, **9**, 193-204.
5. M. Quinten, A. Leitner, J. R. Krenn and F. R. Aussenegg, *Opt. Lett.*, 1998, **23**, 1331-1333.
6. M. L. Brongersma, J. W. Hartman and H. A. Atwater, *Physical Review B*, 2000, **62**, R16356-R16359.
7. S. A. Maier, P. G. Kik, H. A. Atwater, S. Meltzer, E. Harel, B. E. Koel and A. A. G. Requicha, *Nature Materials*, 2003, **2**, 229-232.
8. A. F. Koenderink and A. Polman, *Physical Review B*, 2006, **74**, 033402.
9. D. K. Gramotnev and S. I. Bozhevolnyi, *Nature Photonics*, 2010, **4**, 83-91.
10. N. J. Halas, S. Lal, W.-S. Chang, S. Link and P. Nordlander, *Chemical Reviews*, 2011, **111**, 3932-3934.
11. P. Ben-Abdallah, *Applied Physics Letters*, 2006, **89**, 113117.
12. P. Ben-Abdallah, K. Joulain, J. Drevillon and C. Le Goff, *Physical Review B*, 2008, **77**, 075417.
13. J. Ordonez-Miranda, L. Tranchant, S. Gluchko and S. Volz, *Physical Review B*, 2015, **92**, 115409.
14. E. J. Tervo, O. S. Adewuyi, J. S. Hammonds and B. A. Cola, *Materials Horizons*, 2016, **3**, 434-441.
15. E. Tervo, Z. Zhang and B. Cola, *Physical Review Materials*, 2017, **1**, 015201.
16. W. L. Barnes, A. Dereux and T. W. Ebbesen, *Nature*, 2003, **424**, 824-830.
17. S. Lal, S. Link and N. J. Halas, *Nature Photonics*, 2007, **1**, 641-648.
18. R. M. Dickson and L. A. Lyon, *J Phys Chem B*, 2000, **104**, 6095-6098.
19. T. H. Xiao, Z. Z. Cheng and K. Goda, *Nanotechnology*, 2017, **28**.
20. J. B. Khurgin and A. Boltasseva, *MRS Bulletin*, 2012, **37**, 768-779.
21. J. D. Caldwell, L. Lindsay, V. Giannini, I. Vurgaftman, T. L. Reinecke, S. A. Maier and O. J. Glembocki, *Nanophotonics*, 2015, **4**, 44-68.
22. D. S. Boyuk, L.-W. Chou and M. A. Filler, *ACS Photonics*, 2016, **3**, 184-189.
23. B. M. Kayes, M. A. Filler, M. C. Putnam, M. D. Kelzenberg, N. S. Lewis and H. A. Atwater, *Applied Physics Letters*, 2007, **91**, 103110.
24. L.-W. Chou, N. Shin, S. V. Sivaram and M. A. Filler, *Journal of the American Chemical Society*, 2012, **134**, 16155-16158.
25. L.-W. Chou, D. S. Boyuk and M. A. Filler, *ACS Nano*, 2015, **9**, 1250-1256.
26. C. F. Bohren and D. R. Huffman, *Absorption and Scattering of Light by Small Particles*, Wiley-VCH, Weinheim, 2004.
27. S. Y. Park and D. Stroud, *Physical Review B*, 2004, **69**, 125418.
28. L.-W. Chou, R. D. Near, D. S. Boyuk and M. A. Filler, *The Journal of Physical Chemistry C*, 2014, **118**, 5494-5500.
29. J. Zuloaga and P. Nordlander, *Nano Letters*, 2011, **11**, 1280-1283.
30. Z. M. Zhang, *Nano/Microscale Heat Transfer*, McGraw-Hill, New York, NY, 2007.
31. P. K. Jain, W. Huang and M. A. El-Sayed, *Nano Letters*, 2007, **7**, 2080-2088.
32. S. Underwood and P. Mulvaney, *Langmuir*, 1994, **10**, 3427-3430.
33. T. R. Jensen, M. L. Duval, K. L. Kelly, A. A. Lazarides, G. C. Schatz and R. P. Van Duyne, *The Journal of Physical Chemistry B*, 1999, **103**, 9846-9853.
34. E. Prodan, A. Lee and P. Nordlander, *Chemical Physics Letters*, 2002, **360**, 325-332.
35. K.-S. Lee and M. A. El-Sayed, *The Journal of Physical Chemistry B*, 2006, **110**, 19220-19225.
36. P. K. Jain and M. A. El-Sayed, *Nano Letters*, 2008, **8**, 4347-4352.
37. C. Sonnichsen, B. M. Reinhard, J. Liphardt and A. P. Alivisatos, *Nature Biotechnology*, 2005, **23**, 741-745.
38. A. M. Funston, C. Novo, T. J. Davis and P. Mulvaney, *Nano Letters*, 2009, **9**, 1651-1658.
39. N. Liu, M. Hentschel, T. Weiss, A. P. Alivisatos and H. Giessen, *Science*, 2011, **332**, 1407-1410.
40. B. T. Draine and P. J. Flatau, *J. Opt. Soc. Am. A*, 1994, **11**, 1491-1499.

41. E. D. Palik, *Handbook of Optical Constants of Solids*, Orlando: Academic Press, Orlando, 1985.
42. C. Mätzler, *MATLAB Functions for Mie Scattering and Absorption*, Institut für Angewandte Physik, Bern, Switzerland, 2002.
43. S. Basu, B. J. Lee and Z. M. Zhang, *Journal of Heat Transfer*, 2009, **132**, 023301.
44. J. D. Christesen, C. W. Pinion, E. M. Grumstrup, J. M. Papanikolas and J. F. Cahoon, *Nano Letters*, 2013, **13**, 6281-6286.
45. S. J. Allen, D. C. Tsui and R. A. Logan, *Physical Review Letters*, 1977, **38**, 980-983.
46. T. N. Theis, *Surface Science*, 1980, **98**, 515-532.
47. M. Ferrera, N. Kinsey, A. Shaltout, C. DeVault, V. Shalaev and A. Boltasseva, *J. Opt. Soc. Am. B*, 2017, **34**, 95-103.
48. G. V. Naik, V. M. Shalaev and A. Boltasseva, *Adv Mater*, 2013, **25**, 3264-3294.
49. Y. Zhong, S. D. Malagari, T. Hamilton and D. M. Wasserman, *Journal of Nanophotonics*, 2015, **9**, 093791.
50. M. Hocevar, G. Immink, M. Verheijen, N. Akopian, V. Zwiller, L. Kouwenhoven and E. Bakkers, *Nature Communications*, 2012, **3**, 1266.

An anisotropic nanowire environment around repeated plasmonic resonators improves waveguide performance by up to an order of magnitude.

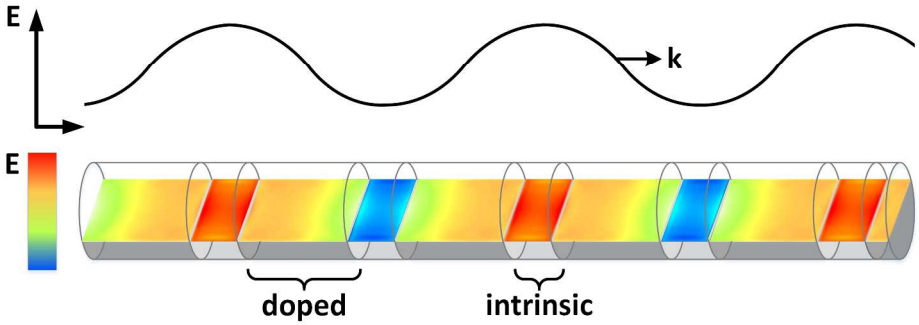

261x116mm (300 x 300 DPI)